

# Exclusive electroproduction of lepton pairs as a probe of nucleon structure

A.V. Belitsky<sup>1</sup>, D. Müller<sup>2,1</sup>

<sup>1</sup>*Department of Physics, University of Maryland, MD 20742-4111, College Park, USA*

<sup>2</sup>*Fachbereich Physik, Universität Wuppertal, D-42097 Wuppertal, Germany*

We suggest the measurement of exclusive electroproduction of lepton pairs as a tool to study inter-parton correlations in the nucleon via generalized parton distributions in the kinematical region where this process is light-cone dominated. We demonstrate how the single beam-spin asymmetry allows to perform such kind of analysis and give a number of predictions for several experimental setups. We comment on other observables which allow for a clean separation of different species of generalized parton distributions.

PACS numbers: 11.10.Hi, 12.38.Bx, 13.60.Fz

Since the discovery of a non-zero spatial extent of the proton in pioneering measurements of electromagnetic form factors [1], the exploration of the hadron's internal structure in terms of quark-gluon degrees of freedom was the subject of intensive theoretical and experimental studies. Until recently, however, only information on one-dimensional slices of the nucleon was extractable from hadronic observables: The spatial charge and magnetization distributions from the form factors alluded to the above; the  $x$ -momentum fraction space parton densities from inclusive reactions, e.g., deeply inelastic scattering of leptons off hadrons [2]. With the realization of the power of exclusive reactions [3], the opportunity of nucleon holography [4] was brought to life; namely, the simultaneous measurement of the longitudinal momentum fraction of partons and their transverse localization within the area of resolution set by the photon virtuality [5] (see also [6, 7]). The corresponding hadronic characteristics, known as generalized parton distributions (GPDs), intertwine the aforementioned conventional hadronic functions. However, they also depend on an extra variable: the  $t$ -channel longitudinal momentum fraction  $\eta$ , the so-called skewedness, which changes the apportion of longitudinal momentum between the absorbed,  $(x - \eta)$ , and created,  $(x + \eta)$ , partons. Thus, GPDs, contrary to conventional Feynman's parton densities, give access to inter-parton correlations rather than mere probabilities through the study of skewedness dependence.

The pioneering experimental study of these new functions at HERMES [8], CLAS [9] and HERA [10] has been done through the exclusive lepton production of the real photon off the proton  $\ell p \rightarrow \ell' \gamma p'$  at high momentum transfer. This process is sensitive to deeply virtual Compton scattering (DVCS) amplitude (see Eq. (4)) parametrized in terms of GPDs. The latter enter also in the lepton production of mesons, i.e.,  $\ell p \rightarrow \ell' M p'$ . Single lepton and nucleon spin asymmetries [11, 12] in the former case allow the direct measurement of GPDs, however, in a very specific kinematics, namely,  $x = -\eta$ . This restriction is a direct consequence of the reality of the outgoing photon. Such a measurement is unable to con-

strain the spin sum rule involving the parton's orbital momentum [13]. Here a process is needed where the momentum fraction varies independently of the skewedness. This can be achieved by the relaxation of the reality condition for the photon in the final state, i.e., by the measurement of lepton pairs produced from a timelike  $\gamma$ -quantum in the elastic electron scattering  $ep \rightarrow e' p' \ell \bar{\ell}$  [12, 14]; see also Ref. [15] for a related reaction.

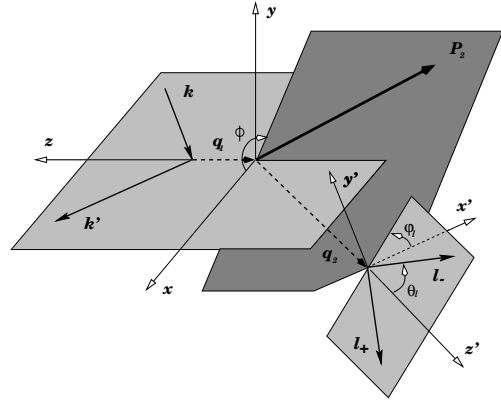


FIG. 1: The kinematics of the lepton pair production in elastic electron scattering off the proton,  $e(k)p(p_1) \rightarrow e(k')p(p_2)\ell(\ell_-)\bar{\ell}(\ell_+)$ , in the fixed target setup.

The differential cross section for the process in the kinematics displayed in Fig. 1 reads

$$d\sigma = \frac{\alpha_{\text{em}}^4}{16(2\pi)^3} \frac{x_B y}{Q^2} |\mathcal{A}|^2 dx_B dy d|\Delta|^2 |d\phi dM_{\ell\bar{\ell}}^2 d\Omega_{\ell}. \quad (1)$$

The incoming photon virtuality and the invariant mass of the lepton pair are  $q_1^2 \equiv -Q^2$  and  $M_{\ell\bar{\ell}}^2 = (\ell_+ + \ell_-)^2$ , respectively. The Bjorken variable and the lepton energy loss is defined conventionally as  $x_B \equiv Q^2/(2p_1 \cdot q_1)$  and  $y \equiv p \cdot q_1/p \cdot k$ .  $\Delta^2 = (p_2 - p_1)^2$  is the  $t$ -channel momentum transfer. The solid angle of the lepton pair in the photon rest frame is  $d\Omega_{\ell} = \sin\theta_{\ell} d\theta_{\ell} d\varphi_{\ell}$ .  $\phi$  is the azimuthal angle between the lepton and hadron scattering planes and plays a distinguished role below. The amplitude  $\mathcal{A}$  represents the sum of the signal in question and

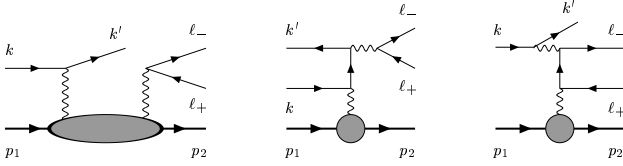


FIG. 2: Contributions to lepton pair production: (from left to right) virtual Compton and Bethe-Heitler processes.

“contaminating” Bethe-Heitler processes,

$$\mathcal{A} = \mathcal{A}_{\text{VCS}} + \mathcal{A}_{\text{BH}_1} + \mathcal{A}_{\text{BH}_2}, \quad (2)$$

corresponding to the first, second and third diagrams in Fig. 2, respectively. The latter two are expressed in terms

of the Dirac and Pauli form factors parametrizing the nucleon matrix element of the quark electromagnetic current,

$$J_\mu = \bar{u}_2 \left( \gamma_\mu F_1 + \frac{i\sigma_{\mu\nu}\Delta_\nu}{2M_N} F_2 \right) (\Delta^2) u_1, \quad (3)$$

with  $u_i$  being the nucleon bispinor  $u_i \equiv u(p_i)$ . As we already mentioned above, they are measurable elsewhere, see, e.g., [16] for the most recent results.

The gauge invariant decomposition of the hadronic tensor contributing to  $\mathcal{A}_{\text{VCS}}$  was found in Ref. [17] by an explicit twist-three analysis at leading order of perturbation theory. To leading twist accuracy, it reads

$$T_{\mu\nu} = i \int d^4z e^{iq \cdot z} \langle p_2 | T \{ j_\mu(z/2) j_\nu(-z/2) \} | p_1 \rangle = \frac{i}{2p \cdot q} \epsilon_{\theta\lambda\rho\sigma} p_\rho q_\sigma \left( g_{\mu\theta} - \frac{p_\mu q_{2\theta}}{p \cdot q_2} \right) \left( g_{\nu\lambda} - \frac{p_\nu q_{1\lambda}}{p \cdot q_1} \right) \mathcal{A}_1(\xi, \eta, \Delta^2) - \frac{1}{2} \left( g_{\mu\nu} - \frac{q_{1\mu} q_{2\nu}}{q_1 \cdot q_2} \right) \mathcal{V}_1(\xi, \eta, \Delta^2) + \frac{1}{2p \cdot q} \left( p_\mu - \frac{p \cdot q_2}{q_1 \cdot q_2} q_{1\mu} \right) \left( p_\nu - \frac{p \cdot q_1}{q_1 \cdot q_2} q_{2\nu} \right) \mathcal{V}_2(\xi, \eta, \Delta^2). \quad (4)$$

Here the symmetrized combinations of momenta  $q \equiv (q_1 + q_2)/2$  and  $p \equiv p_1 + p_2$  are used to define the generalized Bjorken variable  $\xi$  and skewedness parameter  $\eta$ :

$$\xi \equiv -\frac{q^2}{p \cdot q} = x_B \frac{Q^2 - M_{\ell\ell}^2 + \Delta^2/2}{(2 - x_B) Q^2 - x_B (M_{\ell\ell}^2 - \Delta^2)}, \quad (5)$$

$$\eta \equiv \frac{\Delta \cdot q}{p \cdot q} = -\xi \frac{Q^2 + M_{\ell\ell}^2}{Q^2 - M_{\ell\ell}^2 + \Delta^2/2}. \quad (6)$$

Since the light-cone dominance in Eq. (4) is set by the average virtuality  $q^2$  at small  $\Delta^2$  and moderate  $x_B$ , the perturbative QCD approach is applicable provided

$$|q^2| \equiv |Q^2 - M_{\ell\ell}^2 + \Delta^2/2|/2 \gg 1 \text{ GeV}^2. \quad (7)$$

It is lost for  $Q^2 \sim M_{\ell\ell}^2$ , which implies, according to Eq. (5), that  $\xi$  approaches zero. The minimal allowed value is set by  $|\xi_{\min}| \sim 1 \text{ GeV}^2/ys$ , where  $\sqrt{s}$  is the center-of-mass energy. In the light-cone dominated region (7), the Compton form factors factorize into calculable coefficient functions and GPDs. To leading order in coupling constant the Compton form factors satisfy the generalized Callan-Gross relation

$$\mathcal{V}_2 = \xi \mathcal{V}_1. \quad (8)$$

Performing the Dirac decomposition one gets

$$\mathcal{V}_1 = \bar{u}_2 \int dx C_-(x, \xi) \left( \gamma_+ H + \frac{i\sigma_{+\nu}\Delta_\nu}{2M_N} E \right) (x, \eta, \Delta^2) u_1, \\ \mathcal{A}_1 = \bar{u}_2 \int dx C_+(x, \xi) \left( \gamma_+ \gamma_5 \tilde{H} + \frac{\gamma_5 \Delta_+}{2M_N} \tilde{E} \right) (x, \eta, \Delta^2) u_1,$$

in terms of GPDs  $H$ ,  $E$ ,  $\tilde{H}$  and  $\tilde{E}$  [3]. The plus subscript stands for the contraction of the corresponding Lorentz index with the light-like vector  $n_\mu = -\xi(2q_\mu + \xi p_\mu)/q^2$ , which projects out the leading power contribution. From here, one immediately sees the difficulty to measure these functions: one of the dynamical variables enters integrated out with the coefficient function, which reads to leading order in QCD coupling constant,

$$C_\mp(x, \xi) = \frac{1}{\xi - x - i0} \mp \frac{1}{\xi + x - i0}. \quad (9)$$

One can get rid of the convolution provided the observable is sensitive to the imaginary part of the Compton form factors only, i.e.,  $\Im m \mathcal{V}_i$ ,  $\Im m \mathcal{A}_i$ .

The most illuminating experimental observables in this respect are single beam or target spin asymmetries. Their advantage is that they (i) depend linearly on Compton form factors, and (ii) are proportional to their imaginary part. The complete result for the cross section (1), which is represented by a double Fourier sum in azimuthal angles  $d\sigma \sim \sum_{m,n} \cos(m\phi) \{ cc_{m,n} \cos(m\varphi_\ell) + cs_{m,n} \sin(m\varphi_\ell) \} + (\cos \leftrightarrow \sin)$ , will be published elsewhere. Here we limit ourselves to the case of the lepton helicity difference and when one does not distinguish the final state pair with respect to their angular distribution. The integration over the solid angle  $\Omega_\ell$  leads to the vanishing of the interference term  $\mathcal{A}_{\text{VCS}} \mathcal{A}_{\text{BH}_2}^\dagger$  and so the only term which survives in the asymmetry  $\Delta\sigma \equiv \sigma(\lambda = 1) - \sigma(\lambda = -1)$  is  $\mathcal{A}_{\text{VCS}} \mathcal{A}_{\text{BH}_1}^\dagger$ :

$$\frac{d\Delta\sigma}{dx_B dy d|\Delta^2| d\phi dM_{\ell\bar{\ell}}^2} = \frac{2\alpha_{\text{em}}^4}{3\pi} \frac{(2-y)y\sqrt{(1-x_B)Q^2 - x_B M_{\ell\bar{\ell}}^2} \sqrt{\Delta_{\text{min}}^2 - \Delta^2} \sin\phi}{Q^2 M_{\ell\bar{\ell}}^2 \Delta^2 \left( \sqrt{1-y}(Q^2 + M_{\ell\bar{\ell}}^2) + 2(2-y)\sqrt{(1-x_B)Q^2 - x_B M_{\ell\bar{\ell}}^2} \sqrt{\Delta_{\text{min}}^2 - \Delta^2} \cos\phi \right)} \times \left( F_1(\Delta^2) H_s(\xi, \eta, \Delta^2) + \xi(F_1 + F_2)(\Delta^2) \tilde{H}_s(\xi, \eta, \Delta^2) - \frac{\Delta^2}{4M_N^2} F_2(\Delta^2) E_s(\xi, \eta, \Delta^2) \right), \quad (10)$$

where  $F_s(\xi, \eta, \Delta^2) \equiv F(\xi, \eta, \Delta^2) - F(-\xi, \eta, \Delta^2)$ . The minimal value of the  $t$ -channel momentum transfer is  $\Delta_{\text{min}}^2 \approx -4M_N^2\eta^2/(1-\eta^2)$ . The unique feature of the process is that GPDs can be studied as functions of all three arguments independently. Note that if the timelike virtuality is away from the resonance region, the hadronic component of the photon can be neglected and consequently all subprocesses with vector meson production.

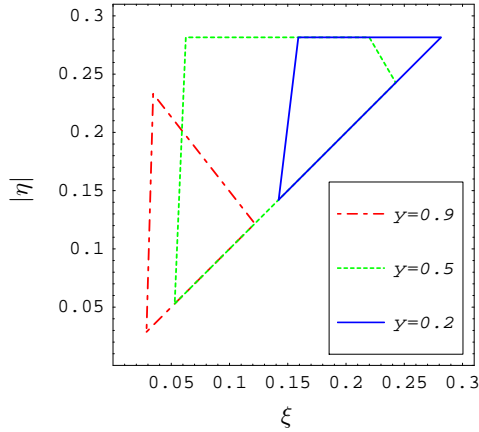


FIG. 3: The  $\xi$ - $\eta$  coverage with  $E = 11$  GeV electron beam. Only the regime  $Q^2 > M_{\ell\bar{\ell}}^2$  is shown. The kinematics is taken as follows:  $\Delta^2 = -0.3 \text{ GeV}^2$ ,  $Q^2$  varies from  $1 \text{ GeV}^2$  to  $4 \text{ GeV}^2$  and  $M_{\ell\bar{\ell}}^2$  from  $0$  to  $Q^2 - 1 \text{ GeV}^2$ . The perimeters of areas covered for different lepton energy losses  $y$  are shown as described in the legend.

As Fig. 3 demonstrates, the region of the GPD surface accessible in this reaction for a fixed target experiment setup is quite extensive. For a given  $\xi$ , cf. Eq. (5), with  $x_B = Q^2/(2M_N E y)$ , the variable  $\eta$  varies in limits

$$\min |\eta| \leq |\eta| \leq \min \{ \max |\eta|, |\eta_{\text{cut}}| \}, \quad (11)$$

where  $\eta$  is evaluated according to Eq. (6) and the bound  $|\eta_{\text{cut}}| \equiv \sqrt{-\Delta^2/(4M_N^2 - \Delta^2)}$  comes from the condition  $|\Delta^2| \geq |\Delta_{\text{min}}^2|$ . The minimal value of  $\xi$  is governed by the requirement of applicability of perturbative QCD treatment, Eq. (7), chosen here as  $Q^2 \geq M_{\ell\bar{\ell}}^2 + 1 \text{ GeV}^2$ . The restriction  $|\eta| \leq \xi$  is a simple consequence of the timelike nature of the final state photon.

The ratio of (10) to the DVCS signal

$$\frac{1}{d\Delta\sigma_{\text{DVCS}}} \int_{4m_e^2}^{Q^2} dM_{\ell\bar{\ell}}^2 \frac{d\Delta\sigma}{dM_{\ell\bar{\ell}}^2} \sim \frac{\alpha_{\text{em}}}{3\pi} \ln \frac{Q^2}{m_e^2}, \quad (12)$$

is of order 0.01 for  $Q^2 \simeq 2 \text{ GeV}^2$ . Difficulties in measuring such a small cross section will be overcome at high-luminosity machines, like JLab@12GeV with  $L = 10^{35} \text{ cm}^{-2} \text{ s}^{-1}$  or in collider experiments due to growth of the cross section with increasing  $\xi$ .

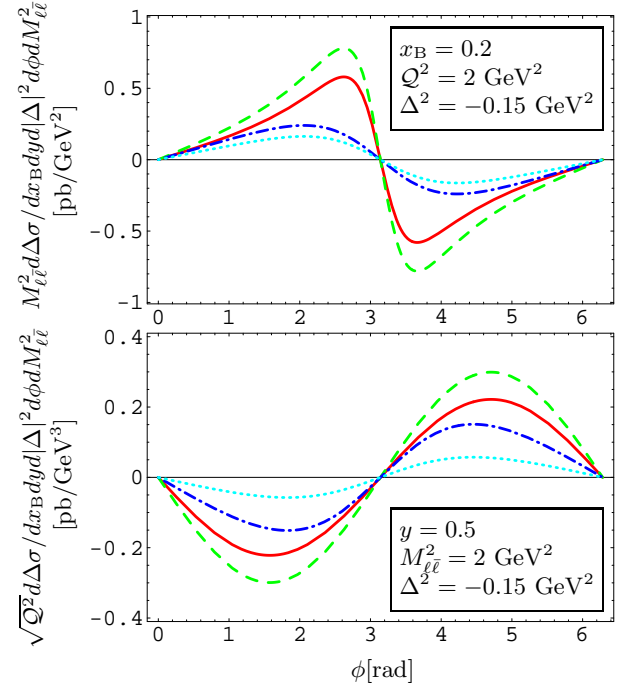


FIG. 4: Azimuthal angle dependence of the scaled cross section of  $e^- p \rightarrow e^- p e^- e^+$  for spacelike (top) and timelike (bottom)  $q^2$  at  $E = 11$  GeV. The solid, dash-dotted and dashed, dotted curves represent predictions for FPD and DD (with  $b = 1$ ,  $B_{\text{sea}} = 9 \text{ GeV}^{-2}$ ) models of Ref. [12], respectively. Top:  $M_{\ell\bar{\ell}}^2 = 0$  for solid, dashed and  $M_{\ell\bar{\ell}}^2 = 0.7 \text{ GeV}^2$  for dashed, dash-dotted curves, respectively. Bottom:  $Q^2 = 0$  for solid, dashed and  $Q^2 = 1 \text{ GeV}^2$  for dash-dotted, dotted curves, respectively.

The cross section (10) being directly proportional to GPDs is extremely sensitive to their skewedness dependence. Such kinds of measurements can easily establish the credibility of our current understanding of mesonic-like components of GPDs and thus constrain the region which is lacking in the establishment of the total spin sum rule [13]. In Fig. 4, we present estimates for JLab@12GeV kinematics using two different models of GPDs: A model without skewedness dependence, which

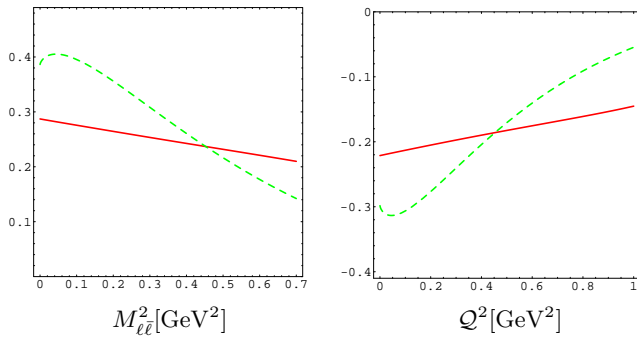


FIG. 5: The dependence of scaled cross section for FPD (solid) and DD (dashed) models at  $\phi = \pi/2$  for  $M_{\ell\ell}^2 d\Delta\sigma$  (left) and  $\sqrt{Q^2} d\Delta\sigma$  (right) for the same kinematical settings as in Fig. 4, top and bottom panels, respectively.

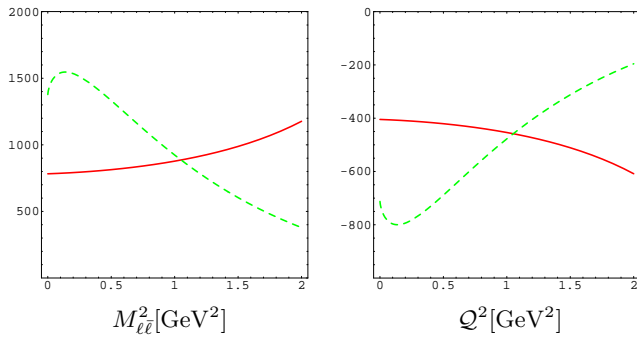


FIG. 6: Same as in Fig. 5, displayed for HERA kinematics with  $y = 0.45$ ,  $\Delta^2 = -0.1 \text{ GeV}^2$ , and  $Q^2 = 4 \text{ GeV}^2$  (left) and  $M_{\ell\ell}^2 = 4 \text{ GeV}^2$  (right).

corresponds to the conventional parton density taken to be the same at all values of  $\eta$ , the so-called forward parton distribution (FPD) model. And a model based on a more sophisticated construction [18] which takes the aforementioned parton densities as input and leads to a nontrivial  $\eta$ -dependence. It is called the double distribution (DD) model. For specific details we refer to Ref. [12]. The most prominent way to discriminate between these models is to study the  $M_{\ell\ell}^2$  or  $Q^2$  dependence of the cross section (10) as shown in Fig. 5. One will be easily able to distinguish between different behaviors by varying the timelike photon virtuality over a short interval below the  $\rho$ -meson threshold. As Fig. 6 shows, the higher energy of HERA results into even higher sensitivity to the skewedness dependence of GPDs. We like to mention that at HERA the skewedness dependence can already be studied in measurements of the unpolarized cross section, since the imaginary part of the Compton amplitude dominates over the real part.

To conclude, the exclusive electroproduction of lepton pairs provides a unique opportunity to determine exhaustive information on the nucleon's internal structure by accessing inter-parton correlations. The underlying GPD can be mapped uniquely as a function of all its variables

which encode dynamics in longitudinal and transverse spaces. Our analysis demonstrates a high sensitivity of the lepton helicity asymmetry to the skewedness dependence of GPDs. Similar conclusions apply to nucleon spin asymmetries which again extract the interference term of Bethel-Heitler and Compton amplitude and separate yet another combination of functions in question. The angular distribution of the final state lepton pairs has a very rich structure and its measurement will lead to an indispensable complementary information on GPDs. One might expect that such studies at collider energies will pin down the skewedness dependence of gluon GPDs in the small- $\xi$  region and thus reduce theoretical uncertainties in diffractive lepton production of vector mesons. Finally, let us point out that the difference between the space- and timelike region is perturbatively computable and so the onset of the light-cone dominance can be elucidated as well.

We would like to thank L. Elouadrhiri, S. Stepanyan and M. Diehl for discussions. Both authors are grateful to the Theory Group and Hall B at Jefferson Lab and D.M. thanks the Nuclear Theory Group at the University of Maryland for the hospitality at the intermediate stages of the work. This work was supported by the US Department of Energy under contract DE-FG02-93ER40762.

- 
- [1] R. Hofstadter, R. McAllister, Phys. Rev. 98 (1955) 217.
  - [2] M. Breidenbach et al., Phys. Rev. Lett. 23 (1969) 935.
  - [3] D. Müller, D. Robaschik, B. Geyer, F.-M. Dittes, J. Horejsi, Fortsch. Phys. 42 (1994) 101; X. Ji, Phys. Rev. D 55 (1997) 7114; A.V. Radyushkin, Phys. Rev. D 56 (1997) 5524; J.C. Collins, L.L. Frankfurt, M. Strikman, Phys. Rev. D 56 (1997) 2982.
  - [4] A.V. Belitsky, D. Müller, Nucl. Phys. A 711 (2002) 118.
  - [5] M. Burkardt, Phys. Rev. D 62 (2000) 071503.
  - [6] J.P. Ralston, B. Pire, hep-ph/0110075.
  - [7] M. Diehl, Eur. Phys. J. C 25 (2002) 223.
  - [8] M. Airapetian, et al. (HERMES Coll.), Phys. Rev. Lett. 87 (2001) 182001.
  - [9] S. Stepanyan et al. (CLAS Coll.), Phys. Rev. Lett. 87 (2001) 182002.
  - [10] C. Adloff et al. (H1 Coll.), Phys. Lett. B 517 (2001) 47.
  - [11] M. Diehl, T. Gousset, B. Pire, J.P. Ralston, Phys. Lett. B 411 (1997) 193; A.V. Belitsky, D. Müller, L. Niedermeier, A. Schäfer, Nucl. Phys. B 593 (2001) 289.
  - [12] A.V. Belitsky, D. Müller, A. Kirchner, Nucl. Phys. B 629 (2002) 323.
  - [13] X. Ji, Phys. Rev. Lett. 78 (1997) 610.
  - [14] M. Guidal, M. Vanderhaeghen, hep-ph/0208275.
  - [15] E.R. Berger, M. Diehl, B. Pire, Eur. Phys. J. C 23 (2002) 675.
  - [16] O. Gayou et al., (Hall A Coll.), Phys. Rev. Lett. 88 (2002) 092301.
  - [17] A.V. Belitsky, D. Müller, Nucl. Phys. B 589 (2000) 611.
  - [18] A.V. Radyushkin, Phys. Rev. D 59 (1999) 014030.